J. metamorphic Geol., 2000, **18**, 409–421

Geochronological constraints on the timing of granitoid magmatism, metamorphism and post-metamorphic cooling in the Hercynian crustal cross-section of Calabria

T. GRAESSNER,[1,2] V. SCHENK,[1] M. BRÖCKER[2] AND K. MEZGER[2]
[1]*Institut für Geowissenschaften der Christian-Albrechts Universität Kiel, 24098 Kiel, Germany (vs@min.uni-kiel.de)*
[2]*Institut für Mineralogie, Zentrallaboratorium für Geochronologie, Universität Münster, 48149 Münster, Germany*

ABSTRACT Exposed cross-sections of the continental crust are a unique geological situation for crustal evolution studies, providing the possibility of deciphering the time relationships between magmatic and metamorphic events at all levels of the crust. In the cross-section of southern and northern Calabria, U–Pb, Rb–Sr and K–Ar mineral ages of granulite facies metapelitic migmatites, peraluminous granites and amphibolite facies upper crustal gneisses provide constraints on the late-Hercynian peak metamorphism and granitoid magmatism as well as on the post-metamorphic cooling. Monazite from upper crustal amphibolite facies paragneisses from southern Calabria yields similar U–Pb ages (295–293 $\pm$ 4 Ma) to those of granulite facies metamorphism in the lower crust and of intrusions of calcalkaline and metaluminous granitoids in the middle crust (300 $\pm$ 10 Ma). Monazite and xenotime from peraluminous granites in the middle to upper crust of the same crustal section provide slightly older intrusion ages of 303–302 $\pm$ 0.6 Ma. Zircon from a mafic to intermediate sill in the lower crust yields a lower concordia intercept age of 290 $\pm$ 2 Ma, which may be interpreted as the minimum age for metamorphism or intrusion. U–Pb monazite ages from granulite facies migmatites and peraluminous granites of the lower and middle crust from northern Calabria (Sila) also point to a near-synchronism of peak metamorphism and intrusion at 304–300 $\pm$ 0.4 Ma. At the end of the granulite facies metamorphism, the lower crustal rocks were uplifted into mid-crustal levels (10–15 km) followed by nearly isobaric slow cooling (*c.* 3 °C Ma^{-1}) as indicated by muscovite and biotite K–Ar and Rb–Sr data between 210 $\pm$ 4 and 123 $\pm$ 1 Ma. The thermal history is therefore similar to that of the lower crust of southern Calabria. In combination with previous petrological studies addressing metamorphic textures and *P–T* conditions of rocks from all crustal levels, the new geochronological results are used to suggest that the thermal evolution and heat distribution in the Calabrian crust were mainly controlled by advective heat input through magmatic intrusions into all crustal levels during the late-Hercynian orogeny.

Key words: Calabria; cooling path; crustal cross-section; U–Pb dating of monazite, xenotime and zircon

INTRODUCTION

Granulite facies metamorphism and associated granitoid magmatism are important processes during the evolution of the continental crust, as they play a dominant role in intracrustal differentiation. These processes have been studied in the exposed crustal cross-section of southern Calabria ever since lower crustal granulite facies metamorphism was found to be synchronous with calcalkaline to metaluminous magmatism in the middle crust (300 $\pm$ 10 Ma) in an area where all levels of a former continental crust are exposed (Schenk, 1980, 1984, 1990). Evidence for internal crustal differentiation processes is the occurrence of peraluminous granites in the middle to upper crust, which, however, show slightly younger ages (293–282 $\pm$ 4 Ma, Rb–Sr whole-rock and mica data; Del Moro *et al.*, 1982). In addition, the observations that mineral growth outlasted deformation both in the upper and the lower crustal rocks, and of elevated geothermal gradients in the lower crust (30–35 °C km^{-1}) and very high gradients in the upper crust (*c.* 60 °C km^{-1}), indicate a strong influence of the granitoid intrusions on the thermal evolution of this crustal section (Schenk, 1984; Graessner & Schenk, 1999).

In contrast to the late-Hercynian ages (310–290 Ma) of the deep crust, upper crustal ortho- and paragneisses possibly record evidence for an early-Hercynian event (330 Ma, Rb–Sr biotite age, Bonardi *et al.*, 1987; poorly constrained lower concordia intercept age of 377 $\pm$ 55 Ma, Schenk, 1990), suggesting that the upper crustal evolution of southern Calabria is more complicated than indicated by geochronological and petrological data. Since none of the data published so far constrain the time of peak metamorphism with enough precision in the upper part of the section, three paragneisses from different levels of the middle to upper crust have been selected for U–Pb monazite and zircon dating. In addition, the relationship between magmatism and metamorphism in the upper and lower crust was addressed by studying monazite from two peraluminous granites that intruded at mid- to upper crustal levels. To further constrain the influence of magmatic rocks on the metamorphism of the lower crustal segment, we have dated a rock of intermediate composition which forms one of the rare intrusive bodies in the metasedimentary sequence of the lower crust.

In the Sila massif of northern Calabria, a large Hercynian unit of granulite facies rocks (*c.* 900 km^2) represents the lower part of the 'Sila nappe' (Fig. 1). The latter shows a similar lithostratigraphic sequence to the crustal section of southern Calabria described above. New petrological studies carried out in the granulite facies part support the interpretation that this unit represents a single segment of a former deep crust (Graessner & Schenk, 2000). Dating of peak metamorphism and determination of the post-metamorphic cooling rate at different levels (top–base) of the former deep crustal segment aims to check the model of a continuous section deduced from petrological data and determine whether it shows the same slow cooling history found in the lower crustal segment of southern Calabria (Schenk, 1980). Additionally, two peraluminous granites have been dated in order to evaluate their chronological relationship to the peak metamorphism in the underlying deep crustal segment.

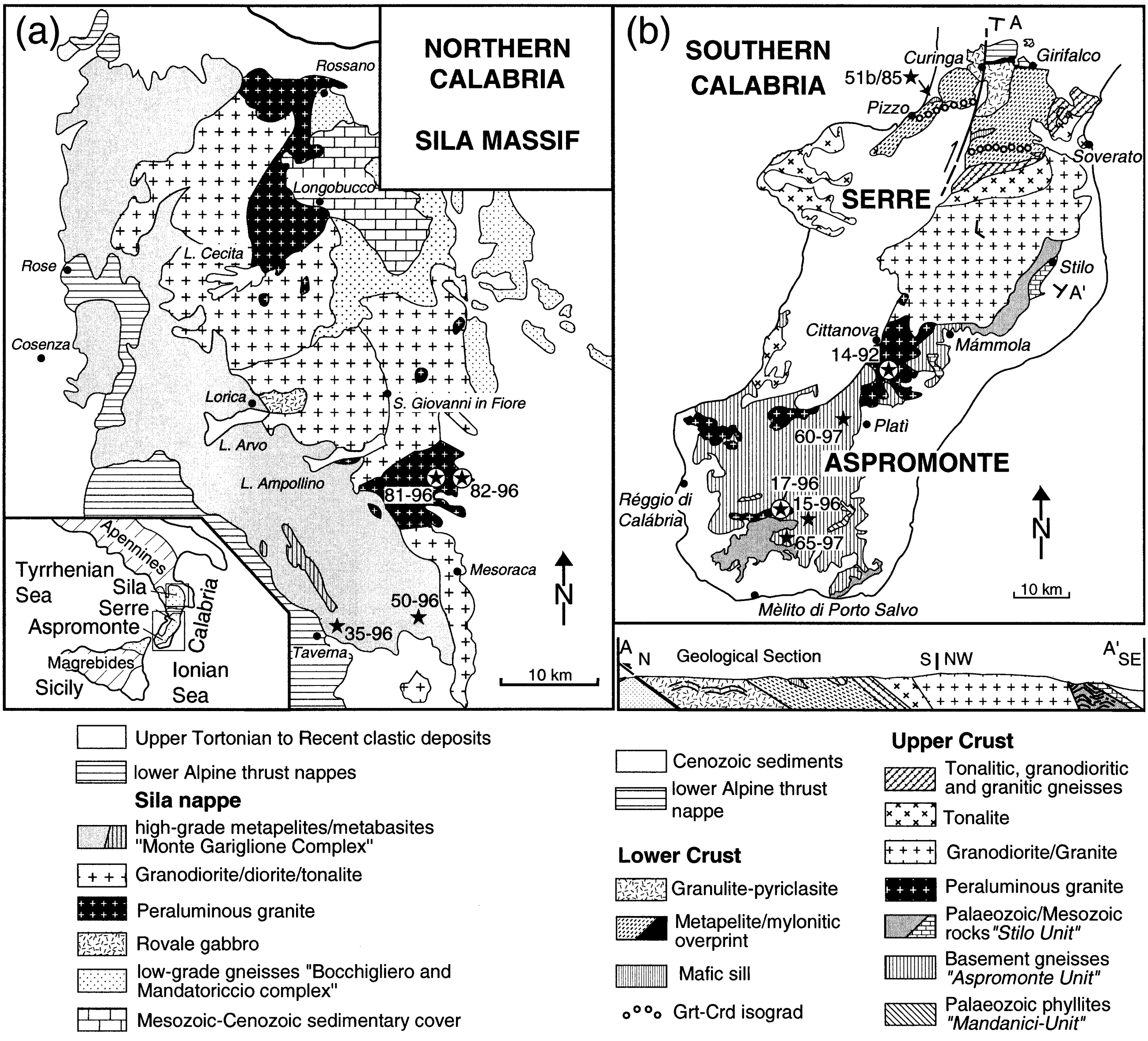

Fig. 1. Simplified geological maps of (a) the Sila massif in northern Calabria (modified after Ayuso *et al.*, 1994), and (b) southern Calabria (modified after Schenk, 1980, 1990; Bonardi *et al.*, 1992). Black stars indicate the locations of samples used for isotopic dating.

The ages of peak metamorphism and the intrusion of the granites have been dated with the U–Pb method on monazite to get an overall comparable dataset for the geological events in all crustal levels of the Serre and the Sila massif during the late-Hercynian orogeny. Monazite is a common accessory in metasedimentary rocks and peraluminous granites, and due to its high closure temperature for the U–Pb system it is very suitable to date high-grade metamorphism and magmatism. Another advantage of monazite is that it generally yields highly precise and concordant U–Pb ages (e.g. Schenk, 1980; Copeland *et al*., 1988; Parrish, 1990; Mezger, 1990; Lanzirotti & Hanson, 1995). Only where no monazite could be found has zircon been used for dating.

Mineral abbreviations are from Kretz (1983).

GEOLOGICAL SETTING OF THE CALABRIAN MASSIF

The Calabrian massif of southern Italy is situated between the thrust belts of the Apennines to the north and the Maghrebides to the west. In contrast to the mainly sedimentary rocks of these mountain belts, the Calabrian massif comprises pre-Alpine continental crust and ophiolitic rocks that were involved in the Alpine orogeny. Due to later movements of microplates in the western Mediterranean, the Alpine mountain system became dismembered (e.g. Alvarez, 1976). Many studies (e.g. Amodio-Morelli *et al*., 1976; Scandone, 1979; Bonardi *et al*., 1982) interpreted the Calabrian massif as a piece of Adriatic or African crust that was overthrust first (Alpidic stage) upon Tethyan ophiolitic units in the north-west. After the collision of Europe with Africa, the Calabrian massif was thrust backwards onto the Apenninic carbonate platform in the east (Apenninic stage). In contrast, Knott (1987), Dietrich (1988), Dewey *et al.* (1989) and Wallis *et al.* (1993) regarded the Calabrian massif as derived from the European continent, thrust eastwards during subduction of the Tethys. As a consequence, it rests now, together with its ophiolitic base, on the Adriatic platform units. However, ophiolitic rocks have not been found in the southern part of the Calabrian massif.

Granulite facies gneisses, exposed in the Serre of southern Calabria (Fig. 1), represent a 7–8 km continuous section through the Hercynian lower continental crust (Schenk, 1980, 1984, 1990). These rocks are overlain by late-Hercynian granitoids, comprising large bodies of metaluminous to calcalkaline tonalites and granodiorites and subordinate peraluminous granites (e.g. D'Amico *et al*., 1982; Rottura *et al*., 1990; Fig. 1). The granitoids intruded into the overlying amphibolite facies upper crustal ortho- and paragneisses ('Aspromonte unit') and low-grade Palaeozoic rocks ('Stilo unit') of the Aspromonte (Fig. 1), which were metamorphosed during Hercynian low-pressure/high-temperature metamorphism (Graessner & Schenk, 1999). Except for a metabasic unit at the base and for two mafic to intermediate sills inside the overlying metapelitic unit, which are only observed in the lower crustal section of southern Calabria, its lithostratigraphy is very similar to that of the Alpine 'Sila nappe' in northern Calabria (e.g. Dubois, 1970, 1976). The simple lithostratigraphic model has been modified by Amodio-Morelli *et al.* (1976), Lorenzoni & Zanettin Lorenzoni (1983) and colleagues who subdivided the high-grade rocks of the Sila into two Alpine units. However, new petrological studies carried out in the Hercynian Monte Gariglione Complex, the lowermost unit, consisting mainly of granulite facies metapelitic migmatites, support the interpretation that the complex represents a continuous section (14–21 km) through a deep segment of the continental crust (Graessner & Schenk, 2000). Peak metamorphic conditions in the lower crustal sections range from 740–770 °C at 4–6 kbar (northern Calabria) and 690–800 °C at 5.5–7.5 kbar (southern Calabria; Schenk, 1984; Graessner & Schenk, 2000). These *P–T* data reveal a slightly higher crustal level for the northern Calabrian segment. Both sections display an unusually high geothermal gradient (35–50 °C km^{-1}) during Hercynian metamorphism which is, however, lower than that deduced from upper crustal rocks in the Aspromonte of southern Calabria (*c.* 60 °C km^{-1}; Graessner & Schenk, 1999).

The sections through the lower crust in northern and southern Calabria reveal similar *P–T* paths. After prograde metamorphism, characterized by strong heating accompanied by moderate loading, a stage of isothermal uplift of the granulite facies lower crustal rocks into mid-crustal levels (10–15 km in northern and 10–18 km in southern Calabria) was followed by nearly isobaric cooling (Schenk, 1984, 1990; Graessner & Schenk submitted).

SAMPLE DESCRIPTION

Northern Calabria

Two samples of the granulite facies metapelitic migmatites of the deep crustal segment were selected to constrain the time of peak metamorphism and the post-peak metamorphic cooling history. Samples were taken from the stratigraphic upper (sample 50-96) and lower parts (sample 35-96) of the deep crustal section (Fig. 1, Table 1). The granulitic segment consists mainly of aluminous paragneisses with interlayered quartzofeldspatic leucosomes. These leucosomes form lenses and bands mostly parallel to the foliation, and are interpreted as partial melts of the host metapelites. Only the melanosomes of the gneisses, consisting of biotite, sillimanite, garnet, quartz and plagioclase, were chosen for geochronology. The metapelites were metamorphosed up to sillimanite + K-feldspar grade; prograde muscovite + quartz was not stable. In sample 50-96, late-stage muscovite + quartz replacing sillimanite + K-feldspar is found, together with retro-

Table 1. Sample locations.

Sample	Location
Northern Calabria	
35-96	Road no. 109 at km 87, west of Magisano
50-96	Road no. 109 at km 110.4, north of Sersale
81-96	At Ponte Coniglio, bridge above the river F. Neto, east of Cotronei
82-96	Private road of the ENEL at the river F. Neto, east of Cotronei
Southern Calabria	
15-96	Bridge above the river F. Amendolea below Roccaforte del Greco
60-97	Banks of the river T. Acone at km 64 along road no. 112 above Platì
65-97	Banks of river T. Pisciato, north of Condofuri
14-92	Eastern entrance of the tunnel Limina at street no. 281, west of Gioiosa Ionica
17-96	Banks of the river F. di Mèlito, north of Bagaladi
51b/85	Road no. 19 at the railway tunnel north of the river F. Angitola, north of Pizzo

grade andalusite and late-stage mats of fibrolitic sillimanite. These reaction textures and mineral phases are typical of the structurally higher parts of the lower crustal section in the Sila massif. Monazite is a common accessory mineral that occurs as inclusions in biotite, plagioclase and in interstices of the rock fabric.

Two different intrusions of peraluminous granite (the so-called 'F. Ampollino' (81-96) and 'Cotronei' granites (82-96); Fig. 1, Table 1) show homogeneous, equigranular textures of quartz, plagioclase and K-feldspar. Additional phases are muscovite and biotite. Cordierite, sillimanite and andalusite were also described from these intrusions (Messina *et al*., 1994). Monazite is common as inclusions in plagioclase and biotite and in interstices of the rock fabric.

Southern Calabria

To decipher the age of metamorphism in the middle to upper crust in the Serre and Aspromonte, three amphibolite facies paragneisses of the 'Aspromonte unit' were collected in the north-east (sample 60-97, middle crust) and in the south (samples 15-96 and 65-97, upper crust) of the Aspromonte (Fig. 1, Table 1). Sample 60-97 consists of prograde biotite, muscovite, quartz and plagioclase and mats of fibrolitic sillimanite overgrowing micas. Deformation of micas and recrystallization of quartz is related to an Alpine overprint which is recorded in this part of the upper crust (30–25 Ma; Bonardi *et al*., 1987). Monazite is common in all parts of the rock and forms inclusions in mica and plagioclase.

Sample 15-96 is an intensely folded paragneiss from the upper crust, with the assemblage biotite, garnet, staurolite, andalusite, muscovite, plagioclase and quartz. Reaction textures (e.g. staurolite inclusions in andalusite) imply that the reaction $St + Ms + Qtz = Bt + And \pm Grt + V$ proceeded, and are similar to textures in the staurolite–andalusite zone of the overlying Stilo unit (Graessner & Schenk, 1999). A difference is the additional occurrence of late-stage fibrolitic sillimanite, overgrowing biotite and muscovite. Monazite occurs as inclusions in biotite, muscovite and plagioclase.

Paragneiss sample 65-97 is from a *c*. 50 cm thick layer rich in garnet–biotite–fibrolite within biotite–plagioclase gneisses. Unfortunately, this rock contained no monazite but small euhedral zircon.

A peraluminous granite ('Punta d'Atò granite'; Fig. 1, Table 1; Messina & Russo, 1981) was sampled in order to constrain the age of intrusion into the upper crust (17-2-96). The rock displays a homogeneous and equigranular texture of quartz, plagioclase and K-feldspar. Additional phases are biotite, muscovite and fibrolitic sillimanite as inclusions in muscovite. Main accessory minerals are monazite and xenotime, included in micas and plagioclase.

A second peraluminous granite ('Cittanova granite', sample 14-92, Fig. 1, Table 1) intruded into the middle crust between the large Serre granodiorite to the north and the gneisses of the Aspromonte unit in the south. It shows a slight foliation and consists of quartz, plagioclase, K-feldspar, muscovite, biotite, ±andalusite, ±fibrolite, ±cordierite and ±garnet (Rottura *et al*., 1986 and references therein).

A metamorphosed lens of a quartz–dioritic intrusion into granulite facies metapelites was sampled (51b/85) from the lower crust. The studied rock is similar to that described and dated by Schenk (1980) as a 250 m thick sill further SE (meta-quartzmonzogabbronorite).

ANALYTICAL PROCEDURES

Monazite, xenotime and zircon ($<350\ \mu m$) were separated from 9–18 kg of fresh rock material using standard techniques (steel jaw-crusher, roller mill, Wilfley table, Frantz magnetic separator, heavy liquids). Prior to dissolution, hand-picked grain size fractions were washed in high purity 2 N HNO_3 (monazite, xenotime) or warm 6 N HNO_3 (zircon), and in high-purity acetone and water to remove any surface contamination. For monazite and xenotime, about 20–60 individual grains were separated. The analysed zircon fraction consists of *c*. 200–600 individual grains. The weight of all grain size fractions was estimated from the shape and density of the individual grains, except for three fractions analysed at the beginning of this study (marked with an asterix in Table 2). In this case, larger grain size fractions were separated and weighed. Dissolution and chemical extraction (anion exchange columns) of U and Pb were performed following Krogh (1973). Most of the monazite and the xenotime fractions were dissolved in 1 ml 6 N HCl and all zircon fractions in 1 ml 24 N HF in Teflon® bombs within screw-top steel containers at 180 °C for 5 days. Only the monazite fractions of samples 35-96 and 82-96 were dissolved in a mixture of 1 ml 6 N HNO_3 : HCl (5 : 1) in Savillex® vials on a hotplate after two weeks. A mixed ^{205}Pb–^{233}U tracer solution was used for isotope dilution, except for one zircon and two monazite grain size fractions (marked with an asterix in Table 2), which were analysed using a mixed ^{208}Pb–^{235}U spike.

Isotope analyses were performed at the 'Zentrallaboratorium für Geochronologie' in Münster using a VG Sector 54 multi-collector mass spectrometer with Daly detector in ion-counting mode (for ^{204}Pb) or using simultaneously Faraday detectors (all other isotopes) and a NBS-type Teledyne mass spectrometer (Rb). U and Pb were loaded on Re filaments with silica gel, H_3PO_4 and 3 N HCl. Measured Pb and U isotopic ratios were corrected for 0.1% and 0.095% fractionation per atomic mass unit, based on repeated analyses of standards NBS SRM 982 and NBS SRM U 500. Total procedural blanks during this study ranged between 0.06 and 0.02 ng Pb. U blanks were not measured since the very low blanks normally obtained are negligible for the high U amounts analysed. The ages and the error ellipses of Table 2 and Fig. 2 were calculated using the recommended IUGS decay constants (Steiger & Jäger, 1977),

Table 2. U–Pb analytical results for monazite, xenotime and zircon from southern and northern Calabria.

Sample[a]	Size (μm)	Rock type	Estimated weight (mg)[b]	Composition[c]			Measured isotopic ratios[d]			Corrected ratios[e]			Correlation coefficient	Apparent ages (Ma)[f]		
				U (ppm)	Pb (ppm)	Common Pb (ng)	$^{206}Pb/^{204}Pb$	$^{208}Pb/^{206}Pb$	$^{207}Pb/^{206}Pb$	$^{206}Pb/^{238}U$	$^{207}Pb/^{235}U$	$^{207}Pb/^{206}Pb$		$^{206}Pb/^{238}U$	$^{207}Pb/^{235}U$	$^{207}Pb/^{206}Pb$
Northern Calabria																
35-96 Mnz	63–80	metapel. migmatite[g]	0.026	3737	1049	0.08	2048 (0.1)	5.734 (0.004)	0.05899 (0.04)	0.04698 (0.18)	0.3390 (0.20)	0.05233 (0.08)	0.82	295.9	296.4 ± 0.5	300.1 ± 0.6
35-96 Mnz	80–100	metapel. migmatite	0.052	3109	818	0.06	4104 (0.2)	5.217 (0.01)	0.05562 (0.04)	0.04809 (0.18)	0.3466 (0.20)	0.05226 (0.07)	0.87	302.8	302.1 ± 0.5	296.9 ± 0.6
50-96 Mnz	63–80	metapel. migmatite	0.023	6135	1234	0.05	5401 (0.1)	3.705 (0.01)	0.05472 (0.02)	0.04851 (0.25)	0.3494 (0.26)	0.05224 (0.05)	0.97	305.4	304.3 ± 0.6	296.1 ± 0.8
50-96 Mnz	80–100	metapel. migmatite	0.04	6078	1105	0.13	4616 (0.2)	3.256 (0.01)	0.05531 (0.03)	0.04838 (0.18)	0.3492 (0.19)	0.05234 (0.06)	0.88	304.6	304.1 ± 0.4	300.5 ± 0.6
81-96 Mnz	63–80	peral. granite[h]	0.029	17806	1308	0.4	3367 (0.1)	0.7150 (0.01)	0.05665 (0.02)	0.04780 (0.26)	0.3455 (0.27)	0.05242 (0.05)	0.97	301.0	301.3 ± 0.6	303.8 ± 0.9
81-96 Mnz	80–100	peral. granite	0.062	7340	894	0.63	2006 (0.1)	1.830 (0.01)	0.05956 (0.01)	0.04827 (0.25)	0.3487 (0.26)	0.05240 (0.06)	0.97	303.9	303.8 ± 0.6	302.9 ± 0.8
82-96 Mnz	80–100	peral. granite	0.027	1563	328	0.05	1644 (0.2)	3.899 (0.01)	0.06071 (0.04)	0.04807 (0.25)	0.3466 (0.27)	0.05229 (0.09)	0.92	302.7	302.1 ± 0.6	298.0 ± 0.8
Southern Calabria																
15-96 Mnz	63–80	paragneiss	0.05	4699	791	0.59	1137 (0.04)	2.999 (0.01)	0.06491 (0.01)	0.04695 (0.18)	0.3380 (0.19)	0.05222 (0.07)	0.86	295.7	295.7 ± 0.5	295.1 ± 0.6
15-96 Mnz	<350	paragneiss	*0.119	*4366	*818	2929 (0.3)	3.647 (0.01)	0.05761 (0.02)	0.04580 (0.30)	0.3323 (0.40)	0.05262	0.77	288.7	291.3 ± 0.4	312.4 ± 0.6	
60-97 Mnz	40–63	paragneiss	0.014	6795	579	0.07	2493 (0.2)	1.214 (0.004)	0.05770 (0.01)	0.04309 (0.25)	0.3099 (0.26)	0.05217 (0.06)	0.96	272.0	274.1 ± 0.5	292.7 ± 0.8
60-97 Mnz	63–80	paragneiss	0.016	5732	524	0.19	1221 (0.1)	1.253 (0.02)	0.06378 (0.02)	0.04492 (0.25)	0.3231 (0.26)	0.05217 (0.07)	0.94	283.2	284.3 ± 0.6	292.8 ± 0.8
65-97 Zrn	<40	paragneiss	0.08	1483	199	0.99	874 (0.6)	0.1573 (0.10)	0.10421 (0.10)	0.12112 (0.63)	1.4771 (0.65)	0.08844 (0.17)	0.96	737.0	921.0 ± 4.0	1392.2 ± 5.0
65-97 Zrn	40–63	paragneiss	0.57	87	12	0.05	5024 (0.2)	0.1291 (0.04)	0.09418 (0.04)	0.13060 (0.19)	1.6522 (0.20)	0.09175 (0.06)	0.89	791.3	990.4 ± 2.0	1462.2 ± 2.0
14-92 Mnz	40–63	peral. granite[h]	0.018	5718	948	0.09	2606 (0.2)	2.886 (0.01)	0.05763 (0.06)	0.04806 (0.20)	0.3468 (0.23)	0.05233 (0.09)	0.88	302.6	302.3 ± 0.6	299.9 ± 0.7
14-92 Mnz	63–80	peral. granite	0.025	4223	703	0.06	3750 (0.1)	2.909 (0.01)	0.05589 (0.02)	0.04815 (0.21)	0.3472 (0.21)	0.05230 (0.06)	0.94	303.1	302.6 ± 0.5	298.4 ± 0.7
17-96 Xen	63–100	peral. granite	0.058	23784	1100	0.34	11434 (0.1)	0.06054 (0.02)	0.05357 (0.01)	0.04821 (0.27)	0.3481 (0.27)	0.05236 (0.05)	0.98	303.5	303.3 ± 0.7	301.4 ± 0.9
17-96 Mnz	<350	peral. granite	*0.153	*16123	*896	12740 (1.3)	0.3192 (0.05)	0.05333 (0.38)	0.04701 (0.52)	0.3382 (0.64)	0.05217	0.80	296.1	295.8 ± 0.8	293.2 ± 0.9	
51b/85 Zrn	<54	basic intrusion	0.198	836	41	0.09	4151 (0.2)	0.1434 (0.01)	0.05611 (0.02)	0.04756 (0.25)	0.3459 (0.26)	0.05274 (0.05)	0.97	299.5	301.6 ± 0.6	317.7 ± 0.8
51b/85 Zrn	54–85	basic intrusion	*0.933	*466	*22	7039 (0.7)	0.1355 (0.02)	0.05448 (0.06)	0.04674 (0.30)	0.3377 (0.30)	0.05240	0.95	294.5	295.5 ± 0.4	303.0 ± 0.5	

[a] Sample name includes the type of mineral (Mnz, monazite; Xen, xenotime; Zrn, zircon). [b] Except for samples marked with an asterix (*), the weight of all grain size fractions was estimated from spheric shape and a density of 5 g cm^{-3} for monazite and 4 g cm^{-3} for zircon. [c] Except for samples marked with an asterix (*), compositions were calculated from estimated weight of grain size fraction[b] [d] Numbers in parentheses are the relative errors (in %) reported at the 2 σ confidence level. [e] Ratios corrected for fractionation, spike, blank and common Pb, as described in the text. Numbers in parentheses are the relative errors (in %) reported at the 2 σ confidence interval. [f] Uncertainty in the apparent ages in million years at the 2 σ confidence interval. [g] metapelitic migmatite. [h] peraluminous granite.

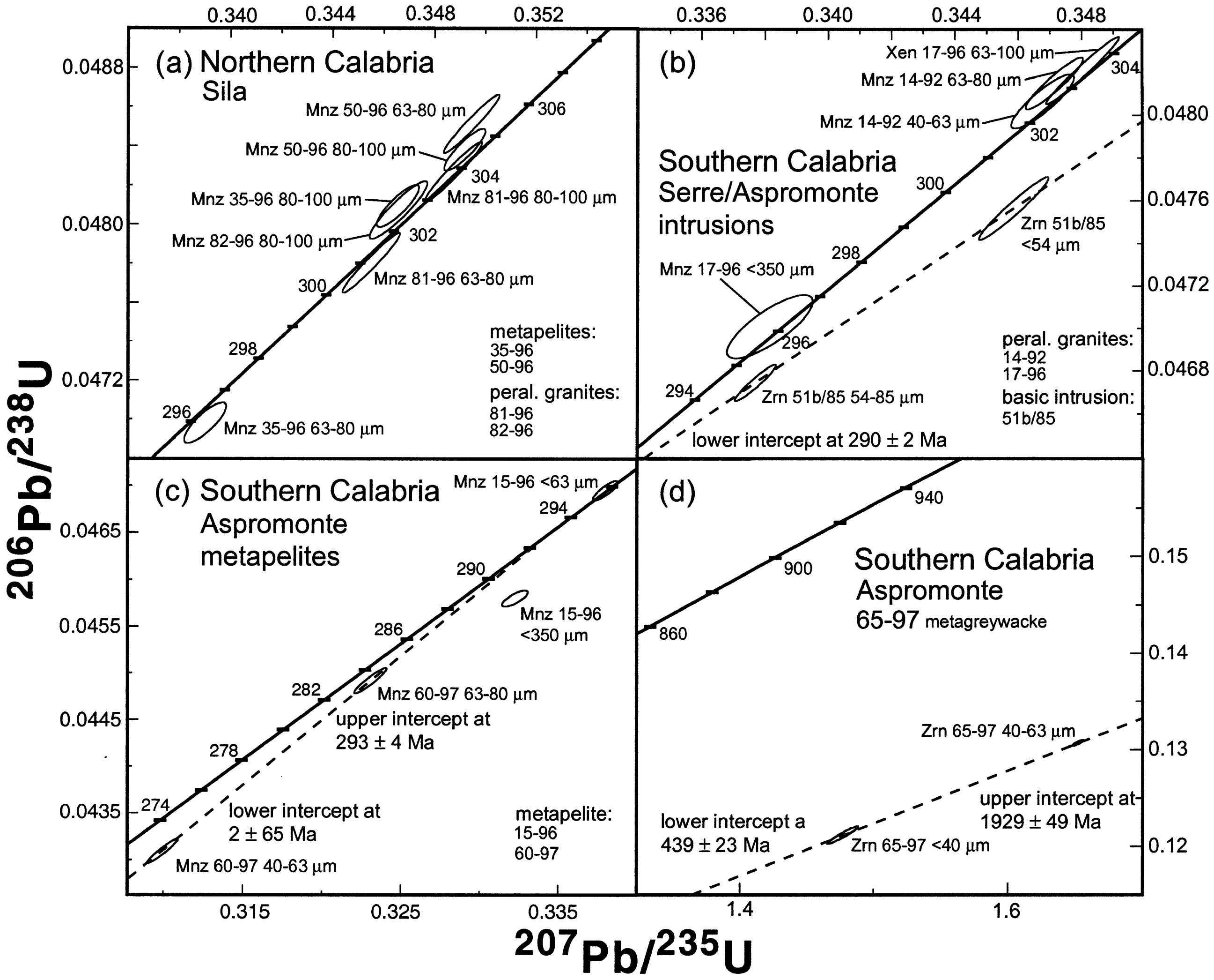

Fig. 2. Concordia diagrams for (a) monazite analyses of granulite facies metapelitic migmatites and peraluminous granites from northern Calabria, (b) monazite, xenotime and zircon data from peraluminous granites from the upper to middle crust and a metabasic intrusion into the lower crust from southern Calabria, (c) monazite data from paragneisses from the upper and middle crust from southern Calabria, and (d) zircon analyses of an amphibolite facies metagreywacke from the upper crust of southern Calabria. Sample number is preceded by the type of mineral dated (Mnz, monazite; Xen, xenotime; Zrn, zircon).

considering the internal 2 σ error of the measurements, the uncertainty in the U–Pb ratio of the spike, the error magnification from the spike/sample ratio and the estimated uncertainty in the isotopic composition of the Pb blank. Measured ratios were corrected for initial isotope Pb composition applying the two-stage model of Stacey & Kramers (1975) using the assumed age of the sample.

Muscovite and biotite were separated from small rock pieces (1–2 kg) of the samples collected for the U–Pb studies. Fractions were enriched in micas using standard techniques (steel jaw-crusher, roller mill, Frantz magnetic separator and adherence to a piece of paper). Only the size fraction 160–200 μm has been considered for Rb–Sr and K–Ar dating. After hand picking, possible contaminants between the mica sheets were removed by grinding under ethanol in an agate mortar. Afterwards, the mica fractions were washed in ethanol and water in an ultrasonic bath.

Whole-rock powder (100 mg) and mica fractions (*c.* 25–40 mg) were mixed with an ^{87}Rb–^{84}Sr tracer solution for isotope dilution prior to dissolution in a mixture of HF:HNO_3 (5:1) in Savillex® vials on a hotplate for 3 days. Chemical extraction of Rb and Sr were performed on cation exchange columns using 2.5 N HCl and loaded on Ta filaments with H_2O or H_3PO_4, respectively. Measured Rb isotopic ratios were corrected for mass fractionation using a factor of 0.9935, determined by repeated measurements of standard NBS SRM 607. Measured Sr ratios were corrected for fractionation based on an ^{86}Sr/^{88}Sr ratio of 0.1194. Repeated runs of standard NBS SRM 987 gave an average ^{87}Sr/^{86}Sr ratio of 0.710265 ± 0.000024 (n = 41). Total blanks for Rb and Sr during the measurements were < 0.05 and 0.1 ng. The uncertainty in ^{87}Rb/^{86}Sr ratios is 1% (2 σ), deduced from repeated measurements. The error in ^{87}Sr/^{86}Sr ratios is based on the internal 2 σ error of the measurements, the estimated uncertainty in the isotopic composition of the spike and the blank, and the error magnification based on the spike/sample ratio. The ages were calculated using the least-square regression technique of York (1969).

K–Ar dating of micas (*c.* 100 mg) was carried out at the 'Institut für Geologie und Dynamik der Lithosphäre, Universität Göttingen'. K was measured by a flame photometer (Eppendorf) and Ar on a VG 1200-C noble gas mass spectrometer. A ^{38}Ar spike with a ^{38}Ar purity of 99.989% was used. The K–Ar ages were calculated using the recommended IUGS decay constants (Steiger & Jäger, 1977).

Back-scattered electron (BSE) and cathodoluminescence (CL) images of monazite, xenotime and zircon were taken on a JEOL Superprobe JXA 8900 RL at the 'Geochemisches Institut, Universität Göttingen', operating at an acceleration voltage of 20 kV and a beam current of 25 nA. BSE images reveal internal compositional variations that are due to contrasts in the average atomic number of elements in the mineral and largely reflect differences in the concentrations of the light rare earth elements, Th, U and Hf (Hanchar & Miller, 1993; Hawkins & Bowring, 1997, 1999). According to these studies, brighter zones of the crystals reflect the higher atomic number and higher Th/U ratios. The CL emission can be enhanced by REE, in particular Dy, Gd, Tb and Y (e.g. Hanchar & Rudnick, 1995).

RESULTS OF U–PB GEOCHRONOLOGY

Northern Calabria

From both samples of metapelitic migmatites, only clear, subhedral to round monazite crystals and some crystal fragments were selected for U–Pb geochronology. Both monazite fractions from sample 50-96 plot slightly above the concordia (Fig. 2a) which can be attributed to the presence of excess ^{206}Pb resulting from the decay of ^{230}Th (Schärer, 1984). In this case, the ^{207}Pb/^{235}U age of 304.1 ± 0.4 Ma is taken as representing the most likely mineral age (Table 2). One grain size fraction of sample 35-96 (80–100 μm) also shows slight reverse discordance, yielding a ^{207}Pb/^{235}U age of 302.1 ± 0.5 Ma (Table 2, Fig. 2a). A second grain size fraction (63–80 μm) of this sample lies slightly discordant below the concordia with an ^{207}Pb/^{206}Pb age of 300.1 ± 0.6 Ma. BSE imaging indicates that some grains of both samples are characterized by continuous to discontinuous growth zoning (Fig. 3a). Other grains have irregular, patchy domains that are truncated by marginal growth zones (Fig. 3b). According to Hawkins & Bowring (1999), these structures might indicate a sequence of precipitation and dissolution of the monazite from a fluid or a melt due to partial melting of the host metapelite during prograde metamorphism. However, some different monazite grains from these samples show homogeneous internal compositional structures. The preservation of nearly concordant and similar ages for most grain size fractions and of the internal structures support the interpretation that monazite reveals the age of crystallization during peak metamorphism. The slight discordance of grain size fraction 63–80 μm of sample 35-96 (Fig. 2a) might indicate minor recent Pb loss. If this monazite fraction also contains excess ^{206}Pb, the resulting ^{207}Pb/^{206}Pb age would be the minimum crystallization age. A different interpretation for the resulting age of this grain size fraction, however, might be a further high-grade metamorphic event at about 296 Ma which cannot strictly be ruled out by the data presented.

From both samples of peraluminous granites, only clear, euhedral elongated to round monazite crystals as well as some fragments were used. The larger size fraction (80–100 μm) of sample 81-96 is nearly concordant and yields a ^{207}Pb/^{235}U age of 303.8 ± 0.6 Ma (Table 2, Fig. 2a). A second fraction of the same sample (63–80 μm) with a ^{207}Pb/^{206}Pb age of 303.8 ± 0.9 Ma plots slightly below the concordia, suggesting that discordance is due to recent radiogenic Pb loss (Fig. 2a). The only studied grain size fraction of sample 82-96 shows a slightly reverse discordance, probably caused by excess thorogenic ^{206}Pb, yielding a ^{207}Pb/^{235}U age of 302.1 ± 0.6 Ma (Table 2, Fig. 2a). BSE images of monazite from all fractions reveal slightly corroded rims and variable internal compositional structures. Some euhedral grains are characterized by concentric growth zoning parallel to crystal faces. They contain deeply resorbed, possibly inherited, xenocrystic oscillatory-zoned cores (Fig. 3c). Other more roundly shaped crystals are irregularly zoned with patchy internal compositional variations (Fig. 3d). Both textures are not only observed in different, but also in the same grain size fractions. Together with their nearly concordant ages, we interpret the internal structures as an indication of episodes of monazite growth and dissolution during emplacement of the granites (cf. Hawkins & Bowring, 1999). The scarcity of possible inherited cores would not have much influence on the crystallization age of monazite.

Southern Calabria

The peraluminous Cittanova (14-92) and Punta d'Atò granites (17-96) contain clear, green–yellow euhedral, well-faceted xenotime (17-96) and yellow, elongated, euhedral to round monazite grains. Both of the monazite fractions of sample 14-92 plot slightly above the concordia, yielding ^{207}Pb/^{235}U ages ranging from 302.6 to 302.3 ± 0.6 Ma (Fig. 2b; Table 2). Most BSE images of sample 14-92 reveal nearly homogeneous internal compositional structures, whereas some monazite grains show irregular, heterogeneous domains truncating the homogeneous part. Xenotime of sample 17-96 (63–100 μm) is slightly reverse concordant, with a ^{207}Pb/^{235}U age of 303.3 ± 0.7 Ma (Fig. 2b; Table 2). BSE images show growth zoning parallel to the crystal shape (Fig. 3e), as well as partially truncated homogeneous cores surrounded by darker euhedral rims. Both structures are interpreted as evidence of crystallization from a melt. A monazite fraction of this sample (<350 μm) plots nearly concordantly with a ^{207}Pb/^{235}U age of 295.8 ± 0.8 Ma (Fig. 2b). This age might be too young compared to the results above, probably reflecting recent Pb loss. If it is assumed that this monazite fraction, like the ones above, contains excess ^{206}Pb, recent Pb loss could have shifted it towards its nearly concordant position. However, it cannot strictly be ruled out that the age of *c.* 296 Ma might reflect a further geological event distinct from that at *c.* 303 Ma.

From two amphibolite facies metapelites of the Aspromonte unit (samples 60-97 & 15-96), clear to slightly clouded, subhedral to ellipsoid-shaped, partly corroded monazite grains and some additional grain fragments were used for U–Pb dating. BSE imaging

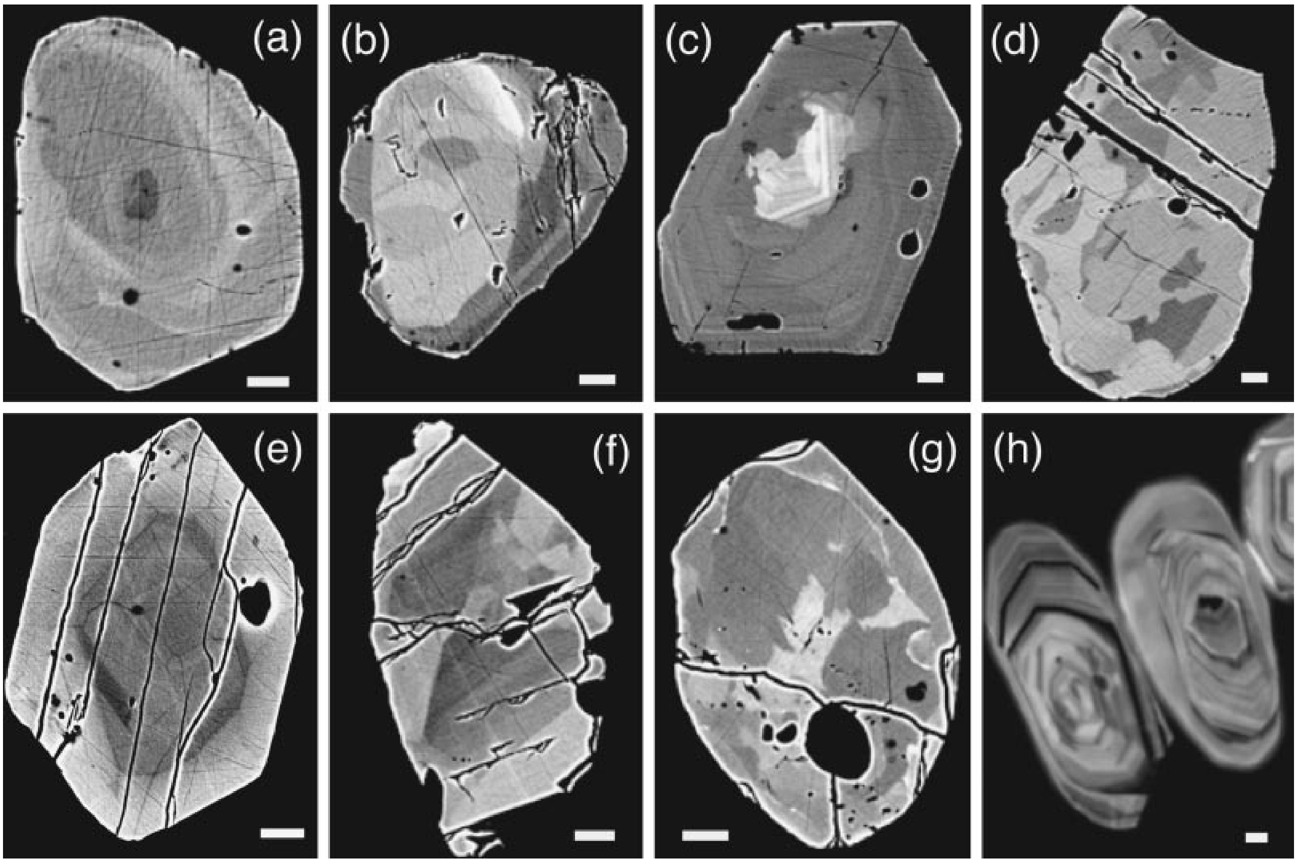

Fig. 3. Back-scattered electron images of monazite crystals from paragneisses ((a) sample 50-96; (b) sample 35-96; (f,g) sample 60-97), peraluminous granite 81-96 (c,d) and a xenotime crystal from the peraluminous granite 17-96 (e). Cathodoluminscence image of zircon crystals from a quartz–dioritic intrusion 51b/85 (h). The scale bar is 10 μm in every image. For further discussion see text.

indicates internal compositional variations as described above. Monazite from each fraction shows homogeneous compositions to patchy irregular zoning as well as some truncated and partly resorbed regular zones in the cores (Fig. 3f,g). Both monazite fractions of sample 60-97 plot strongly discordantly below the concordia (Fig. 2c, Table 2), possibly as a result of Pb loss induced by an Alpine overprint at 30–25 Ma reported in that area (Bonardi *et al.*, 1987). The monazite fractions define an upper intercept age of about 293 ± 4 Ma, which is similar to the $^{207}Pb/^{206}Pb$ ages of both fractions of 292.7 ± 0.8 Ma (Table 2) and is interpreted as the age of amphibolite facies metamorphism. The irregularly truncated domains in weakly zoned cores might reflect the growth of secondary monazite due to the Alpine overprint (Fig. 3f). Since one monazite fraction of sample 15-96 (63–80 μm) yields concordant ages of 295.7 ± 0.5 Ma (Table 2, Fig. 2c), a peak metamorphic origin of all compositional variations is more likely. The second grain fraction (<350 μm) of sample 15-96 with a $^{207}Pb/^{206}Pb$ date of 312.4 ± 0.6 Ma plots strongly discordantly below concordia, suggesting recent Pb loss (Fig. 2c). The ages discussed above might also be interpreted as minimum ages of the peak metamorphic event if it is assumed that the monazite, like that of the peraluminous granites, originally plotted above the concordia due to the presence of excess ^{206}Pb.

Two fractions of small, clear, elongated euhedral to slightly rounded zircon grains of a metamorphosed quartz–dioritic sill (51b/85) are discordant and define a lower intercept age of 290 ± 2 Ma (Fig. 2b). BSE and CL images reveal in most cases fine-scale magmatic zoning patterns. Some grains show perhaps partially resorbed relic cores with magmatic zoning (Fig. 3h). Slightly rounded crystals indicate a late, nearly homogeneous, overgrowth which cuts and truncates the magmatic cores described above. Since the zircon has high U concentrations (400–860 ppm), they might have been more susceptible to metamictization than grains with lower U contents and therefore also to recent differential Pb loss. Recent Pb loss would have resulted in a rotation of the discordia to a lower meaningless intercept age (cf. Mezger & Krogstad, 1997). The lower intercept at 290 ± 2 Ma would therefore indicate the minimum age of the dated event. The geological interpretations of the lower and upper discordia intercepts are not unequivocal. On the one hand, the upper intercept might be the magmatic crystallization, the lower intercept the metamorphism. However, it may also be that the upper intercept is caused by an inherited component, whereas the lower intercept reflects the time of magmatic crystallization and metamorphism in the lower crust.

Two analysed grain size fractions of very small ($< 63\ \mu$m) zircon from the paragneiss 65-97 of the amphibolite facies upper crust defines an obviously meaningless lower intercept age of 439 ± 23 Ma (Fig. 2d). This age is as poorly constrained as the lower concordia intercept age of zircon from a paragneiss of the upper crust (377 ± 55 Ma; Schenk, 1990).

RESULTS OF RB–SR AND K–AR GEOCHRONOLOGY

The results of Rb–Sr and K–Ar dating on muscovite and biotite (Tables 3 and 4) are used to constrain the cooling history of the granulite facies rocks of the Sila massif. Since the closure temperatures for the Rb–Sr system are higher than those of the K–Ar system for biotite and muscovite, the Rb–Sr system is expected to give older ages. Additionally, the closure temperature for the Rb–Sr and the K–Ar systems in muscovite is significantly higher than in biotite. The closure temperature for Rb–Sr in muscovite has been estimated at *c.* 500 ± 50 °C, and in biotite at *c.* 350 °C (Hanson & Gast, 1967; Purdy & Jäger, 1976; Dodson, 1979). The closure temperature for K–Ar in muscovite is *c.* 350 ± 40 °C and in biotite it is *c.* 280 ± 40 °C (Purdy & Jäger, 1976; Harrison *et al.*, 1985). Thus, corresponding ages indicate the time of cooling for the temperature range *c.* 500 to 300 °C.

For the granulite facies metapelitic migmatites from northern Calabria, the Rb–Sr method (biotite–whole rock) indicates ages of 123 ± 1 Ma (sample 35-96) and 189 ± 2 Ma (sample 50-96) (Table 3). The age difference is consistent with the different structural levels of the samples (Fig. 1). During cooling, the closure temperature for biotite will be reached earlier in the upper, colder parts of the crust than in deeper structural levels. The K–Ar biotite ages for the same samples are consistent with this interpretation, even though the first K–Ar age is slightly older than the corresponding Rb–Sr age: 128.2 ± 2.6 Ma for sample 35-96 and 175.2 ± 3.6 Ma for sample 50-96 (Table 4).

For sample 50-96, muscovite dating defines an Rb–Sr age of 287 ± 8 Ma (Table 3) and a K–Ar age of 209.9 ± 4.5 Ma (Table 4). The latter is similar to an Rb–Sr age (muscovite–plagioclase) of 203 ± 4 Ma of a granulite facies aplitic sill in the lower crust of southern Calabria (Schenk, 1980). Therefore, it is concluded that the K–Ar age reflects the cooling age of the muscovite after Hercynian granulite facies metamorphism, whereas the Rb–Sr age does not seem to be of any geological significance. A possible explanation would be a disturbance of the Rb–Sr system of the whole rock by infiltration of late-stage Rb-rich fluids from the nearby granites. This would have increased the ^{87}Rb/^{86}Sr ratio of the whole rock and therefore also the muscovite–whole rock age. In this case, the effect on the biotite–whole rock age would be minor due to the higher ^{87}Rb/^{86}Sr ratio of the biotite (421.5) compared to muscovite (4.635).

COMPARISON WITH PREVIOUS STUDIES AND TEMPERATURE–TIME HISTORY

U–Pb monazite dating of granulite facies metapelitic migmatites and of peraluminous granites of the Sila massif in northern Calabria yields similar ages of 304–300 ± 0.4 Ma for the time of lower crustal metamorphism and of granite intrusion into the middle crust. Our study provides ages for the late-Hercynian emplacement of the granites which are *c.* 8–15 Myr older than the dates of Ayuso *et al.* (1994) who reported cooling ages of 293–289 ± 1 Ma (^{40}Ar/^{39}Ar of muscovite and hornblende) from various types of peraluminous and calcalkaline granitoids. A similar situation occurs for age data from southern Calabria, where a previous study (Del Moro *et al.*, 1982) reported Rb–Sr biotite and muscovite ages for the peraluminous granite of Cittanova (291–284 ± 4 Ma)

Table 3. Rb–Sr isotope analyses used for mineral dating of metapelitic migmatites from the lower crust of northern Calabria.

Sample	Type	Rb (ppm)	Sr (ppm)	^{87}Rb/^{86}Sr[a]	^{87}Sr/^{86}Sr[a,b]	Initial ^{87}Sr/^{86}Sr	Age (Ma)[c]
35-96	Whole rock	57.0	270.4	0.611	0.72433 (0.004)		
	Biotite	245	9.898	72.66	0.85009 (0.005)	0.723	123 ± 1
50-96	Whole rock	128	214.4	1.727	0.72124 (0.003)		
	Biotite	392	2.989	421.5	1.84899 (0.006)	0.717	189 ± 2
	Muscovite	162	101.4	4.635	0.73313 (0.007)	0.714	287 ± 8

[a] Ratios corrected for fractionation, spike and blank as described in the text. [b] Numbers in parentheses are the relative errors (in %) reported at the 2 σ confidence interval. [c] Uncertainty in ages in million years at the 2 σ confidence interval.

Table 4. K–Ar analytical results from biotite and muscovite of metapelitic migmatites from the lower crust of northern Calabria.

Sample	Mineral	Spike (no.)	K_2O (wt%)	^{40}Ar (nl/g)	^{40}Ar (%)	Age (Ma)[a]
35-96	Biotite	2308	8.93	38.24	98.97	128.2 ± 2.6
50-96	Muscovite	2318	7.72	55.40	98.61	209.9 ± 4.5
50-96	Biotite	2311	8.77	52.00	99.34	175.2 ± 3.6

[a] Uncertainty in ages in million years at the 2 σ confidence level. Dating by H. Arendt, Institut für Geologie und Dynamik der Lithosphäre, Universität Göttingen.

that are lower than the monazite U–Pb ages of 303–302 ± 0.6 Ma obtained in this study.

For the first time, monazite ages of two paragneisses of the upper crust of southern Calabria ('Aspromonte unit') are reported here. One concordant monazite and an upper concordia intercept yield ages of 295 ± 0.6 and 293 ± 4 Ma. From this it is evident that peak metamorphism in the upper crust was attained at the same time as in the lower part of this crustal section, dated with monazite at 296–290 ± 2 Ma (Schenk, 1980). Concordant monazite ages at 296–290 ± 2 Ma and the lower intercept ages of zircon of granulite facies metapelites, felsic granulites and metabasites of the lower crust at 295–292 ± 2 and 312 ± 10 Ma are similar to the intrusion ages of tonalites and dioritic gneisses of the middle crust (295–293 ± 2 Ma) and of the Serre granodiorite (< 314 Ma) of the upper crust (Schenk, 1980, 1990). Dating of discordant zircon from an intermediate sill in the lower crust yields a lower intercept age of *c.* 290 ± 2 Ma, which can either be interpreted as the time of metamorphism or as the minimum age of intrusion, if inherited lead is the reason for discordance. The latter scenario has also been proposed for a comparable basic intrusion in the lower crust where nearly concordant zircon provided ages of 298 ± 5 Ma (Schenk, 1980).

In this study, U–Pb ages of monazite are interpreted to reflect the time of growth and recrystallization during peak metamorphism. Petrological studies have shown that, during peak metamorphism in the lower crust, temperatures of 700–800 °C were attained in southern and 740–770 °C in northern Calabria (Schenk, 1984, 1990; Graessner & Schenk, 2000). These temperatures are in the range of or above those (700–750 °C) at which many authors assume that monazite in a dry system retains its U–Pb isotopic signature (Copeland *et al.*, 1988; Parrish, 1990; Mezger *et al.*, 1991, 1993). If monazite ages reflect cooling below a closure temperature of *c.* 700–750 °C, samples from the lower crustal section in southern Calabria, which have experienced peak metamorphic temperatures of 800 °C, would be expected to have younger monazite ages than rocks from the upper part of this section, where only *c.* 700 °C has been attained (Schenk, 1980, 1990). It can be argued that very fast uplift has caused the matching ages for metamorphic rocks affected by different peak temperatures. However, this can definitely be ruled out because available data indicate a cooling rate of 2 °C Ma^{-1} (Schenk, 1980, 1990). Therefore, it is concluded that monazite records the time of peak metamorphic crystallization. This assumption is supported by similar data from Sila which show no correlation between lithostratigraphic position, i.e. peak metamorphic temperatures, and monazite ages. Recent findings by DeWolf *et al.* (1993), Spear & Parrish (1996) and Bingen & van Breemen (1998) in high-grade metamorphic terranes, as in earlier studies on Calabria (Schenk, 1980, 1990), all support closure temperatures for the U–Pb system in monazite that are significantly above 700 °C.

Ages determined for monazite from amphibolite facies paragneisses from the middle to upper crust are also interpreted to reflect crystallization. This is in accordance with the studies of Smith & Barreiro (1990) and Kingsbury *et al.* (1993) which documented monazite growth at temperatures corresponding to the staurolite-in isograd.

In contrast to the results of U–Pb dating, the K–Ar and Rb–Sr ages of biotite and muscovite obtained from metapelitic migmatites of the Sila massif are much younger than the late-Hercynian metamorphic event and are therefore interpreted as cooling ages. This conclusion is supported by the fact that younger mineral ages were recorded at the base than at the top of the lower crustal segment.

The scenario of post-Hercynian slow cooling of granulite facies gneisses from the Sila at mid-crustal levels (10–15 km depth; Fig. 4), resembles that deduced for the lower crust in southern Calabria (Schenk, 1980, 1990). According to petrological data, the latter crustal section isobarically cooled at a deeper crustal level (12–18 km) after metamorphism, which is in agreement with the younger cooling ages of biotite in the Serre (135–110 Ma) than in the Sila massif (189–123 Ma). Borsi & Dubois (1968) reported Rb–Sr biotite and muscovite ages of rocks from the base of the lower crustal section of the Sila nappe. The biotite ages scatter between 205 and 103 Ma, and the muscovite ages between 253 and 210 Ma, which is in the range of the mineral ages obtained in the present study. Supplementary cooling ages in the Serre of feldspar (Rb–Sr), hornblende (K–Ar) and garnet (Sm–Nd) give a good constraint on the regular slow cooling (*c.* 2 °C Ma^{-1}) of this lower crustal section (Schenk, 1990). This cooling rate is similar to that indicated by the mica data obtained from the Sila.

Constraints on the final uplift of the lower crustal section in the Sila massif to surface level are given by apatite and zircon fission track ages from Thomson (1994). As for Rb–Sr and K–Ar ages of micas, higher apatite and zircon fission track ages were obtained for rocks from the structurally upper part (19 & 45 Ma, respectively) than for those from the structurally lower part (17 & 21–24 Ma, respectively) (Fig. 4). Thomson (1994, 1998) interpreted these ages as reflecting exhumation due to late-orogenic extension and synchronous erosion during the Oligocene to Miocene. This process follows continuous NW-directed subduction of the Tethys below the Calabrian massif, which gave rise to elevated cooling rates of 5–13 °C Ma^{-1} between > 45 Ma and *c.* 15 Ma. Cooling of the exposed lower crustal rocks must have ceased at about 11 Ma ago, which accounts for the oldest age of Tortonian sediments resting on top of the Calabrian lower crustal rocks (van Dijk & Okkes, 1991).

CONCLUSIONS

The ages of amphibolite and granulite facies metamorphism of upper crustal paragneisses, lower crustal

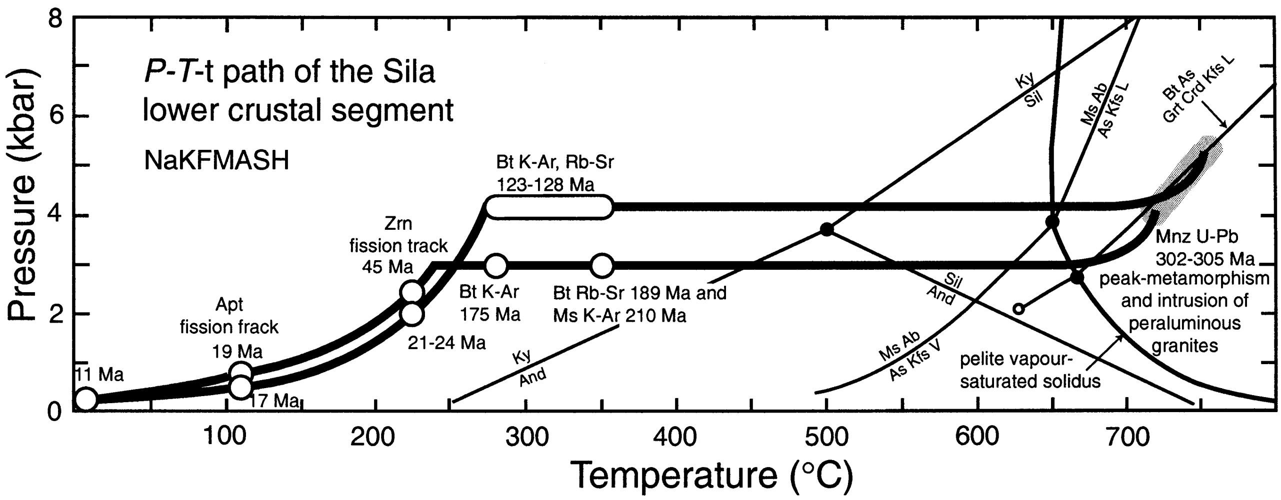

Fig. 4. *P–T–t* path of the lower and upper part of the lower crustal segment of the Sila massif in northern Calabria. The grey area shows *P–T* conditions in the granulite facies lower crust during peak metamorphism (Graessner & Schenk submitted). Final uplift of the lower crustal section is deduced from apatite and zircon fission track data of Thomson (1994) and the oldest overlying sediments of Tortonian age (11 Ma). Reaction curves and invariant points in the NaKFMASH system after Spear *et al.* (1999). Closure temperatures of micas are given in the text, those for apatite and zircon fission track ages are $110\pm10\,^{\circ}$C (Green *et al.*, 1989) and $225\pm25\,^{\circ}$C (Hurford, 1991), respectively. See text for further discussion.

metapelitic migmatites and intrusions of peraluminous granites into the middle crust of northern and southern Calabria were isotopically dated in this study. In the Sila massif of northern Calabria, monazite yielded similar U–Pb ages of $304–300\pm0.4$ Ma for the granulite facies metamorphism and for non-metamorphic peraluminous granites which intruded into the middle crust. Emplacement ages for granites of southern Calabria (Serre, Aspromonte) are similar ($303–302\pm0.6$ Ma) and fall into the range between 310 and 290 Ma obtained for the granulite and the amphibolite facies metamorphism in different levels of the crust, and for calcalkaline to metaluminous granitoids from other parts of the crustal profile (Schenk, 1980, 1990, and this study).

Previous petrological studies adressing the metamorphic evolution of southern Calabria have shown that the deformation–crystallization relationship during the prograde metamorphic evolution is similar in the upper and the lower parts of the crust (Schenk, 1984, 1990; Graessner & Schenk, 1999). The peak metamorphic assemblages grew mainly syntectonically during late-Hercynian metamorphism, but mineral growth outlasted the deformation. However, the main difference refers to the prograde evolution of the lower crust which is characterized by a pressure increase not seen in the upper crustal rocks. The new data presented here support the interpretation that this might be caused by the large calcalkaline (quartz–diorites and tonalites) to peraluminous granitoid intrusions into the middle crust which certainly provoked metamorphic heating and contributed to the loading of the lower crust and crustal thickening synchronously with metamorphism (Schenk, 1980, 1990; Graessner & Schenk, 1999). These granitoids possibly provided the heat for the late static metamorphic stage in all crustal levels and caused the relatively small temperature difference between the base of the upper crust (620 °C at *c.* 2.5 kbar) and the top of the lower crust (690 °C at 5.5 kbar) (Schenk, 1984; Graessner & Schenk, 1999). A paleo-geotectonic setting of a continental arc above a subduction zone would satisfy the petrological and isotopic data for the Calabrian massif.

The same geotectonic setting can account for the Sila massif of northern Calabria. A petrological study of the lower crustal gneisses has shown a late static mineral growth that is best documented in metabasic rocks (Graessner & Schenk submitted). Together with the dated synchronism of geological events, the granulite facies metamorphism in the lower crust can be related to the intrusions of the peraluminous granites into the middle crust. As in southern Calabria, fast uplift of the lower granulite facies segment into mid-crustal levels (10–15 km) was followed by slow cooling of *c.* 3 °C Ma^{-1} (Fig. 4). Whether the granite intrusions have affected the thermal conditions in the upper crust of the Sila massif as in southern Calabria remains to be determined in the future.

ACKNOWLEDGEMENTS

We thank H. Baier and S. Rochnowski (Münster) for help in the laboratory and on the mass spectrometers. A. Kronz (Universität Göttingen) is thanked for assistance with BSE and CL images on the microprobe. The paper benefited from constructive reviews by S. Jung and an anonymous reviewer, and the careful editorial handling of D. Robinson. The Deutsche Forschungsgemeinschaft supported the project through grant Sche 265/9-2.

REFERENCES

Alvarez, W., 1976. A former continuation of the Alps. *Bulletin of the Geological Society of America*, **87,** 891–896.

Amodio-Morelli, L., Bonardi, G., Colonna, V. *et al.*, 1976. L'arco Calabro-Peloritano nell'orogene Appeninico-Maghrebide. *Memorie della Societá Geologia Italiana*, **17,** 1–60.

Ayuso, R. A., Messina, A., De Vivo, B., Russo, S., Woodruff, L. G., Sutter, J. F. & Belkin, H. E., 1994. Geochemistry and argon thermochronology of the Variscan Sila batholith, southern Italy: source rocks and magma evolution. *Contributions to Mineralogy and Petrology*, **117,** 87–109.

Bingen, B. & van Breemen, O., 1998. U–Pb monazite ages in amphibolite- to granulite-facies orthogneiss reflect hydrous mineral breakdown reactions: Sveconorwegian province of SW Norway. *Contributions to Mineralogy and Petrology*, **132,** 336–353.

Bonardi, G., De Vivo, B., Giunta, G., Lima, A., Perrone, V. & Zuppetta, A., 1982. Mineralizzazioni dell'Arco Calabro-Peloritano. Ipotesi genetiche e quadro evolutivo. *Bolletino della Società Geologia Italiana*, **101,** 141–155.

Bonardi, G., Compagnoni, R., Del Moro, A., Messina, A. & Perrone, V., 1987. Riequilibrazioni tettono-metamorfiche alpine nell'Unita dell'Aspromonte, Calabria meridionale. *Rendiconti Società Italiana di Mineralogia e Petrologia*, **42,** 301.

Bonardi, G., Compagnoni, R., Messina, A., Perrone, V., Russo, S., De Francesco, A. M., Del Moro, A. & Platt, J., 1992. Sovrimpronta metamorfica alpina nell'Unità dell'Aspromonte (settore meridionale dell'Arco Calabro-Peloritano). *Bolletino della Società Geologia Italiana*, **111,** 81–108.

Borsi, S. & Dubois, R., 1968. Données géochronologiques sur l'histoire hercynienne et alpine de la Calabre centrale. *Comptes Rendus de l'Académie des Sciences de Paris*, **266,** 72–75.

Copeland, P., Parrish, R. R. & Harrison, T. M., 1988. Identification of inherited radiogenic Pb in monazite and its implications for U–Pb systematics. *Nature*, **333,** 760–763.

D'Amico, C., Rottura, A., Maccarone, E. & Puglisi, G., 1982. Peraluminous granitic suite of Calabria-Peloritani Arc (southern Italy). *Rendiconti Società Italiana di Mineralogia e Petrologia*, **38,** 35–52.

Del Moro, A., Pardini, G., Maccarrone, E. & Rottura, A., 1982. Studio radiometrico Rb–Sr di granitoidi peraluminosi dell'Arco Calabro-Peloritano. *Rendiconti Società Italiana di Mineralogia e Petrologia*, **38,** 1015–1026.

Dewey, J. F., Helman, M. L., Turco, E., Hutton, D. W. H. & Knott, S. D., 1989. Kinematics of the western Mediterranean. In: *Alpine Tectonics* (eds Coward, M. P. & Dietrich, D.), *Geological Society of London Special Publication*, **45,** 265–283.

DeWolf, C. P., Belshaw, N. & O'Nions, R. K., 1993. A metamorphic history from micron-scale $^{207}Pb/^{206}Pb$ chronometry of Archean monazite. *Earth and Planetary Science Letters*, **114,** 207–220.

Dietrich, D., 1988. Sense of overthrust shear in the Alpine nappes of Calabria (Southern Italy). *Journal of Structural Geology*, **10,** 373–381.

Dodson, M. H., 1979. Theory of cooling ages. In. *Lectures in Isotope Geology* (eds Jäger, E. & Hunziker, J. C.), pp. 194–202. Springer, New York.

Dubois, R., 1970. Phase de serrage, nappes de socle et métamorphisme alpin a la jonction calabre-apennin: la suture calabro-apenninique. *Revue de Géographie Physique et de Géologie Dynamique*, **12,** 221–253.

Dubois, R., 1976. La suture Calabro-Apenninique Cretace-Eocene et L'ouverture Tyrrhenienne Neogene: etude petrographique et structurale de la Calabre centrale. *Doctorate Thesis, Université Pierre et Marie Curie*, *Paris.*

Graessner, T. & Schenk, V., 1999. Low-pressure metamorphism of Palaeozoic pelites in the Aspromonte, southern Calabria. Constraints for the thermal evolution in the Calabrian cross-section during the Hercynian orogeny. *Journal of Metamorphic Geology*, **17,** 157–172.

Graessner, T. & Schenk, V., 2000. An exposed Hercynian lower crustal section in the Sila massif of northern Calabria: mineral chemistry, petrology and a *P–T* path of granulite facies metapelitic migmatites and metabasites. *Journal of Petrology*, in press.

Green, P. F., Duddy, I. R., Laslett, G. M., Hegarty, K. A., Gleadow, A. J. W. & Lovering, J. F., 1989. Thermal annealing of fission tracks in apatite 4. Qualitative modelling techniques and extensions to geological timescales. *Chemical Geology*, **79,** 155–182.

Hanchar, J. M. & Miller, C. F., 1993. Zircon zonation patterns as revealed by cathodoluminescence and backscattered electron images: implications for interpretation of complex crustal histories. *Chemical Geology*, **110,** 1–13.

Hanchar, J. M. & Rudnick, R. L., 1995. Revealing hidden structures: the application of cathodoluminescence and back-scattered electron imaging to dating zircons from lower crustal xenoliths. *Lithos*, **36,** 289–303.

Hanson, G. N. & Gast, P. W., 1967. Kinetic studies in contact metamorphic zones. *Geochimica et Cosmochimica Acta*, **31,** 1119–1153.

Harrison, T. M., Duncan, I. & McDougall, I., 1985. Diffusion of ^{40}Ar in biotite: temperature, pressure and compositional effects. *Geochimica et Cosmochimica Acta*, **49,** 2461–2468.

Hawkins, D. P. & Bowring, S. A., 1997. U–Pb systematics of monazite and xenotime: case studies from the Paleoproterozoic of the Grand Canyon, Arizona. *Contributions to Mineralogy and Petrology*, **127,** 87–103.

Hawkins, D. P. & Bowring, S. A., 1999. U–Pb monazite, xenotime and titanite geochronological constraints on the prograde to post-peak metamorphic thermal history of Paleoproterozoic migmatites from the Grand Canyon, Arizona. *Contributions to Mineralogy and Petrology*, **134,** 150–169.

Hurford, A. J., 1991. Uplift and cooling pathways derived from fission track analysis and mica dating: a review. *Geologische Rundschau*, **80,** 349–368.

Kingsbury, J. A., Miller, C. A., Wooden, J. L. & Harrison, T. M., 1993. Monazite paragenesis and U–Pb systematics in rocks of the eastern Mojave Desert, California, U.S.A: implications for thermochronometry. *Chemical Geology*, **110,** 147–167.

Knott, S. D., 1987. The Liguride Complex of southern Italy—a Cretaceous to Paleogene accretionary wedge. *Tectonophysics*, **142,** 217–226.

Kretz, R., 1983. Symbols for rock-forming minerals. *American Mineralogist*, **68,** 277–279.

Krogh, T. E., 1973. A low-contamination method for hydrothermal decomposition of zircon and extraction of U and Pb for isotopic age determinations. *Geochimica et Cosmochimica Acta*, **37,** 485–494.

Lanzirotti, A. & Hanson, G. N., 1995. U–Pb dating of major and accessory minerals formed during metamorphism and deformation of metapelites. *Geochimica et Cosmochimica Acta*, **59,** 2513–2526.

Lorenzoni, S. & Zanettin Lorenzoni, E., 1983. Note illustrative della carta geologica della Sila alla scala 1 : 200.000. *Memorie della Societá Geologia Italiana*, **36,** 317–342.

Messina, A. & Russo, S., 1981. I graniti peraluminosi del versante meridionale dell'Aspromonte (Calabria). *Bolletino della Società Geologia Italiana*, **100,** 3–14.

Messina, A., Russo, S., Borghi, A., Colonna, V., Compagnoni, R., Caggianelli, A., Fornelli, A. & Piccareta, G., 1994. Il massico della Sila settore settentrionale dell'arco Calabro-Peloritano. Guida all'escursione del gruppo 'I basamenti cristallini e i granitoidi circum-mediterranei: evoluzione petrogenetica e implicazioni geodinamiche'. *Bolletino della Società Geologia Italiana*, **113,** 539–586.

Mezger, K., 1990. Geochronology in granulites. In: *Granulites and Crustal Evolution* (eds Vielzeuf, D. & Vidal, P. H.), pp. 451–470. Kluwer Academic Publishers, Dordrecht, The Netherlands.

Mezger, K. & Krogstad, E. J., 1997. Interpretation of discordant U–Pb zircon ages: an evaluation. *Journal of Metamorphic Geology*, **15,** 127–140.

Mezger, K., Rawnsley, C. M., Bohlen, S. R. & Hanson, G. N., 1991. U–Pb garnet, sphene, monazite and rutile ages: implications for the duration of high-grade metamorphism and cooling histories, Adirondack Mts., New York. *Journal of Geology*, **99,** 415–428.

Mezger, K., Essene, E. J., van der Pluijm, B. A. & Halliday, A. N., 1993. U–Pb geochronology of the Grenville Orogen of Ontario and New York: constraints on ancient crustal tectonics. *Contributions to Mineralogy and Petrology*, **114,** 13–26.

Parrish, R. R., 1990. U–Pb dating of monazite and its application to geological problems. *Canadian Journal of Earth Sciences*, **27,** 1431–1450.

Purdy, J. W. & Jäger, E., 1976. K–Ar ages on rock-forming minerals from the Central Alps. *Memoirs of the Institute of Geology and Mineralogy, University of Padova*, **30,** 1–31.

Rottura, A., Atzori, P., Bargossi, G. M. *et al*., 1986. *The late Hercynian granitoids from southern sectors of Calabrian Arc (southern Italy). Excursion guide to the annual field meeting of 'Granitologues'*. Istituto di Mineralogia e Petrografia, Università di Bologna, Bologna.

Rottura, A., Bargossi, G. M., Caironi, V. *et al*., 1990. Petrogenesis of contrasting Hercynian granitoids from the Calabrian Arc, southern Italy. *Lithos*, **24,** 97–119.

Scandone, P., 1979. Origin of the Tyrrhenian Sea and Calabrian Arc. *Bolletino della Società Geologia Italiana*, **98,** 27–34.

Schärer, U., 1984. The effect of initial ^{230}Th disequilibrium on young U–Pb ages: the Makalu case, Himalaya. *Earth and Planetary Science Letters*, **67,** 191–204.

Schenk, V., 1980. U–Pb and Rb–Sr radiometric dates and their correlation with metamorphic events in the granulite-facies basement of the Serre, southern Calabria (Italy). *Contributions to Mineralogy and Petrology*, **73,** 23–38.

Schenk, V., 1984. Petrology of felsic granulites, metapelites, metabasics, ultramafics, and metacarbonates from southern Calabria (Italy): prograde metamorphism, uplift and cooling of a former lower crust. *Journal of Petrology*, **25,** 255–298.

Schenk, V., 1990. The exposed crustal cross section of southern Calabria, Italy: structure and evolution of a segment of Hercynian crust. In: *Exposed Cross-Sections of the Continental Crust* (eds Salisbury, M. H. & Fountain, D. M.), pp. 21–42, Kluwer, Dordrecht, The Netherlands.

Smith, H. & Barreiro, B., 1990. Monazite U–Pb dating of staurolite grade metanorphism in pelitic schists. *Contributions to Mineralogy and Petrology*, **105,** 602–615.

Spear, F. S. & Parrish, R. R., 1996. Petrology and cooling rates of the Valhalla complex, British Columbia, Canada. *Journal of Petrology*, **37,** 733–765.

Spear, F. S., Kohn, M. J. & Cheney, J. T., 1999. *P–T* paths from anatectic pelites. *Contributions to Mineralogy and Petrology*, **134,** 17–32.

Stacey, J. S. & Kramers, J. D., 1975. Approximation of terrestrial lead isotope evolution by a two-stage model. *Earth and Planetary Science Letters*, **26,** 207–221.

Steiger, R. H. & Jäger, E., 1977. Subcommision on Geochronology: convention on the use of decay constants in geo- and cosmochronology. *Earth and Planetary Science Letters*, **36,** 359–362.

Thomson, S. N., 1994. Fission track analysis of the crystalline basement rocks of the Calabrian Arc, southern Italy: evidence of Oligo-Miocene late-orogenic extension and erosion. *Tectonophysics*, **238,** 331–352.

Thomson, S. N., 1998. Assessing the nature of tectonic contacts using fission-track thermochronology: an example from the Calabrian Arc, southern Italy. *Terra Nova*, **10,** 32–36.

van Dijk, J. P. & Okkes, F. W. M., 1991. Neogene tectonostratigraphy and kinematics of Calabrian basins: implications for the geodynamics of the Central Mediterranean. *Tectonophysics*, **196,** 23–60.

Wallis, S. R., Platt, J. P. & Knott, S. D., 1993. Recognition of syn-convergence extension in accretionary wedges with examples from the Calabrian Arc and the Eastern Alps. *American Journal of Science*, **293,** 463–494.

York, D., 1969. Least squares fitting of a straight line with correlated errors. *Earth and Planetary Science Letters*, **5,** 320–324.

Received 10 September 1999; revision accepted 16 February 2000.